



AFRL-RZ-WP-TP-2010-2252

CAVITY COUPLED AERORAMP INJECTOR COMBUSTION STUDY (POSTPRINT)

Dell T. Olmstead, Mark R. Gruber, and MacKenzie J. Collatz

**Propulsion Sciences Branch
Aerospace Propulsion Division**

Richard D. Branam

Air Force Institute of Technology

Kuo-Cheng Lin

Taitech, Inc.

AUGUST 2009

Approved for public release; distribution unlimited.

See additional restrictions described on inside pages

STINFO COPY

**AIR FORCE RESEARCH LABORATORY
PROPULSION DIRECTORATE
WRIGHT-PATTERSON AIR FORCE BASE, OH 45433-7251
AIR FORCE MATERIEL COMMAND
UNITED STATES AIR FORCE**

REPORT DOCUMENTATION PAGE				<i>Form Approved</i> OMB No. 0704-0188	
The public reporting burden for this collection of information is estimated to average 1 hour per response, including the time for reviewing instructions, searching existing data sources, gathering and maintaining the data needed, and completing and reviewing the collection of information. Send comments regarding this burden estimate or any other aspect of this collection of information, including suggestions for reducing this burden, to Department of Defense, Washington Headquarters Services, Directorate for Information Operations and Reports (0704-0188), 1215 Jefferson Davis Highway, Suite 1204, Arlington, VA 22202-4302. Respondents should be aware that notwithstanding any other provision of law, no person shall be subject to any penalty for failing to comply with a collection of information if it does not display a currently valid OMB control number. PLEASE DO NOT RETURN YOUR FORM TO THE ABOVE ADDRESS.					
1. REPORT DATE (DD-MM-YY) August 2009		2. REPORT TYPE Conference Paper Postprint		3. DATES COVERED (From - To) 01 August 2008 – 31 August 2009	
4. TITLE AND SUBTITLE CAVITY COUPLED AERORAMP INJECTOR COMBUSTION STUDY (POSTPRINT)				5a. CONTRACT NUMBER In-house	
				5b. GRANT NUMBER	
				5c. PROGRAM ELEMENT NUMBER 62203F	
6. AUTHOR(S) Dell T. Olmstead, Mark R. Gruber, and MacKenzie J. Collatz (AFRL/RZAS) Richard D. Branam (Air Force Institute of Technology) Kuo-Cheng Lin (Taitech, Inc.)				5d. PROJECT NUMBER 3012	
				5e. TASK NUMBER AI	
				5f. WORK UNIT NUMBER 3012AI00	
7. PERFORMING ORGANIZATION NAME(S) AND ADDRESS(ES) <div style="display: flex; justify-content: space-between;"> <div style="width: 45%;"> Propulsion Sciences Branch (AFRL/RZAS) Aerospace Propulsion Division Air Force Research Laboratory, Propulsion Directorate Wright-Patterson Air Force Base, OH 45433-7251 Air Force Materiel Command, United States Air Force </div> <div style="width: 45%;"> Air Force Institute of Technology (AFIT/ENY) 2950 Hobson Way Wright-Patterson AFB, OH 45433-7765 ----- Taitech, Inc. 1430 Oak Court, Suite 301 Beavercreek, OH 45430 </div> </div>				8. PERFORMING ORGANIZATION REPORT NUMBER AFRL-RZ-WP-TP-2010-2252	
9. SPONSORING/MONITORING AGENCY NAME(S) AND ADDRESS(ES) Air Force Research Laboratory Propulsion Directorate Wright-Patterson Air Force Base, OH 45433-7251 Air Force Materiel Command United States Air Force				10. SPONSORING/MONITORING AGENCY ACRONYM(S) AFRL/RZAS	
				11. SPONSORING/MONITORING AGENCY REPORT NUMBER(S) AFRL-RZ-WP-TP-2010-2252	
12. DISTRIBUTION/AVAILABILITY STATEMENT Approved for public release; distribution unlimited.					
13. SUPPLEMENTARY NOTES Conference paper published in the <i>Proceedings of the 45th AIAA/ASME/SAE/ASEE Joint Propulsion Conference and Exhibit</i> , conference held August 2 - 5, 2009 in Denver, CO. This paper contains color. PA Case Number: 88ABW-2009-3064; Clearance Date: 06 Jul 2009. The U.S. Government is joint author of this work and has the right to use, modify, reproduce, release, perform, display, or disclose the work.					
14. ABSTRACT The objective of this study was to provide a direct comparison between the single angled injector and the aeroramp injector arrays in such a combustion environment. Ignition limits and pre-combustion shock position were used to define the operability differences while combustion efficiency and stream thrust were used for performance comparisons. These parameters were determined by operating a scramjet combustor in dual-mode operation over the range of Mach numbers expected during scramjet takeover from a boost vehicle. Performance and operability conclusions are based on raw data from static pressures, temperature measurements, and thrust stand loading. It was determined that the operability reduces significantly for the aeroramp injector for all conditions tested, but the performance is virtually identical to that of the round injectors. The aeroramp injector performance indicated improved near-field combustion with the potential for better performance in higher Mach number flow to include full supersonic combustion mode for which it was designed.					
15. SUBJECT TERMS supersonic combustion, fuel injection, flameholding					
16. SECURITY CLASSIFICATION OF:			17. LIMITATION OF ABSTRACT: SAR	18. NUMBER OF PAGES 22	19a. NAME OF RESPONSIBLE PERSON (Monitor) Mark R. Gruber 19b. TELEPHONE NUMBER (Include Area Code) N/A
a. REPORT Unclassified	b. ABSTRACT Unclassified	c. THIS PAGE Unclassified			

Cavity Coupled Aeroramp Injector Combustion Study

Dell T. Olmstead,¹ Mark R. Gruber,² and MacKenzie J. Collatz³
Air Force Research Laboratory, Wright Patterson AFB, OH, 45433

Richard D. Branam⁴
Air Force Institute of Technology, Wright Patterson AFB, OH 45433

and

Kuo-Cheng Lin⁵
Taitech Inc., Beavercreek, OH, 45430

The difficulties with fueling of supersonic combustion ramjet engines with hydrocarbon based fuels presents many challenges. The need for a better solution to supersonic mixing has led to the development of many different styles of fuel injection. An aerodynamic ramp injector has been shown to have a quantitative improvement over a physical ramp while still achieving desirable mixing characteristics. Little quantitative combustion data is available on the performance of aerodynamic ramp injectors in a cavity-coupled scramjet flowpath, especially relative to round injectors. The objective of this study was to provide a direct comparison between the single angled injector and the aeroramp injector arrays in such a combustion environment. Ignition limits and pre-combustion shock position were used to define the operability differences while combustion efficiency and stream thrust were used for performance comparisons. These parameters were determined by operating a scramjet combustor in dual-mode operation over the range of Mach numbers expected during scramjet takeover from a boost vehicle. Performance and operability conclusions are based on raw data from static pressures, temperature measurements, and thrust stand loading. It was determined that the operability reduces significantly for the aeroramp injector for all conditions tested, but the performance is virtually identical to that of the round injectors. The aeroramp injector performance indicated improved near-field combustion with the potential for better performance in higher Mach number flow to include full supersonic combustion mode for which it was designed.

Nomenclature

I-1	=	Injector 1
I-2	=	Injector 2
I-5	=	Injector 5
I-6	=	Injector 6
I_{sp}	=	Specific impulse
P_{T4}	=	Combustor entrance total pressure (kPa)
T_{T5}	=	Combustor entrance total temperature (kPa)
P_5	=	Combustor exit pressure (kPa)
Q	=	Dynamic pressure (kPa)
W_a	=	Air mass flow rate (kg/s)
W_f	=	Fuel mass flow rate (kg/s)

¹ AFIT MS Student and Deputy Branch Chief, Aerospace Propulsion Technology Branch, AIAA Member

² Senior Aerospace Engineer, Aerospace Propulsion Science Branch, AIAA Associate Fellow

³ AFIT MS Student and Deputy Branch Chief, Aerospace Propulsion Science Branch, AIAA Member

⁴ Assistant Professor, Department of Aeronautics and Astronautics, AIAA Associate Member

⁵ Sr. Research Scientist, Taitech Inc., AIAA Senior Member

η_c = Combustion efficiency
 Φ = Equivalence ratio, phi

L/D or L_{cav}/D = Cavity length to depth ratio
 L_{isol}/H or L/H = Ratio of Length of Isolator to Throat Height

I. Introduction

ACHIEVING optimal mixing in a supersonic combustor ramjet (scramjet) is an extremely challenging task due to the need for rapid injection and mixing due to the one-millisecond class residence times. This challenge is exaggerated because the rapid mixing must be done while generating the minimum aerodynamic and thermodynamic losses in a high speed environment where total pressure, static temperature, and thus efficiency are very sensitive to flow disruptions that would aid mixing.

In small scramjet engines with about 4.5 kg/s (10 lbm/s) air mass flow, conventional angled wall injectors can be used to achieve satisfactory mixing. Vehicles using this size engine are greatly limited in total size so the engine must be scaled up to a size that is useful for missions such as long range reconnaissance and space-lift vehicles that could have air mass flow closer to 450 kg/s(100 lbm/s.) Current injection styles will be insufficient to achieve proper mixing in such large flowpaths. Many different styles of injectors have been developed to address this challenge to include struts, swept physical ramps, aerodynamic ramps, slots, and arrays of injectors.^{1,2,3} The aerodynamic ramp (aeroramp) injector utilizes the tailored interaction of the plumes from an array of wall fuel injectors to achieve some of the mixing benefits of the intrusive devices, but at a much lower cost in total pressure and thermodynamic load. An improved aeroramp design was developed by Jacobsen et al.⁴ that greatly simplified the original aeroramp design and mitigated some concerns about fuel trapped on the wall.

The aerodynamic ramp injector has been analyzed in Mach 2.0, 2.4, and 4.0 cross-flows using both CFD and experiments.^{4,5,6,7} Many of these experiments specifically focused on the aerodynamic ramp coupled with a plasma torch for the ignition of the scramjet engine. Several recent tests have incorporated a cavity flameholder,⁸ dual-mode combustion backpressure, and combustion,⁹ but not all in the same test.

II. Experimental Method

A. Test Article

The experiment was performed on the thrust stand inside Research Cell 18 (RC-18) at Wright-Patterson Air Force Base. This facility was designed for fundamental studies of supersonic reacting flows using a continuous-run direct-connect open-loop airflow supported by the Research Air Facility. The test rig consists of a natural-gas-fueled vitiator, interchangeable facility nozzles (Mach-1.8 and 2.2 currently available), modular isolator, modular combustor, and exhaust, as illustrated in Figure 1. The rig is mounted to a thrust stand capable of measuring thrust up to 9 kN (~2000 lbf).

The facility air supply is capable of providing up to 13.6 kg/s (30 lb/s) of air, with total pressures and temperatures up to 51 atm (750 psia) and 900 K (~1600 R), respectively. An exhaust system with a pressure as low as 0.24 atm (3.5 psia) lowers and maintains the backpressure for smooth starting and safe operation. Combined with currently available Mach-1.8 and 2.2 facility nozzles, the air vitiator was fine-tuned to simulate discrete flight conditions from Mach 3.5 to 5 at flight dynamic pressures up to 96 kPa (2000 psf) (Table 1). The relatively low simulated flight Mach numbers represent the scramjet takeover conditions, at which dual-mode combustion takes place.

Table 1. Simulated flight conditions and fueling schemes.

Case	Flight M	Flight Q	Φ (I-2)	Φ (I-5 or I-6)
1	5	48	0.6	0
2	5	48	0.9	0
3	5	48	0.6	0.3
4	4.5	48	0.6	0
5	5	48	0.6	0.3
6	4.5	48	0.6	0.3
7	4	96	0.3	0.3
8	4	96	0.3	0.3
9	3.5	48	0.3	0.3
10	3.5	48	0.3	0.6
11	3.5	48	0.3	0.3
12	3.5	48	0.3	0.6

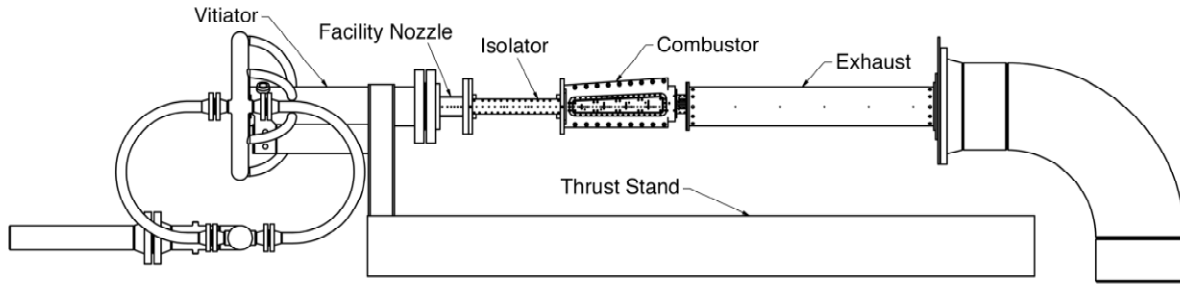


Figure 1. Schematic of Research Cell 18 combustion facility at WPAFB.

The scramjet flow path of the present study shown in Figure 1 consists of a heat-sink rectangular isolator and a rectangular combustor featuring a recessed cavity flame holder and flush-wall injectors. The isolator has a rectangular cross-section with a height of 38.1 mm (1.5 in), a width of 101.6 mm (4.0 in), and a length of 654 mm (25.75 in). The combustor has a total length of 914 mm (36 in) and a constant divergence angle of 2.6 degrees. Figure 2a illustrates the entire flow path and the arrangement of crucial components. A thermal barrier coating covers the interior surface of the entire flow path for additional thermal protection. Two water-cooled combustor sidewall inserts can be replaced with quartz windows for flame visualization and optical measurements.

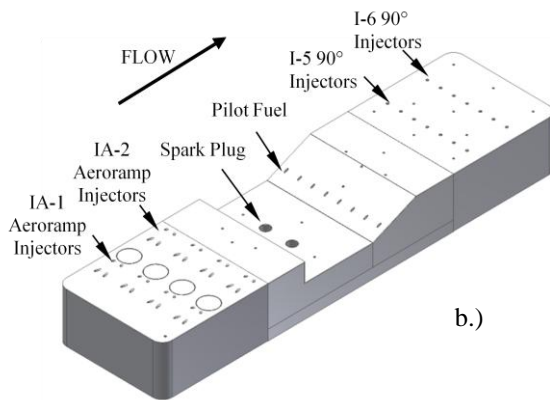
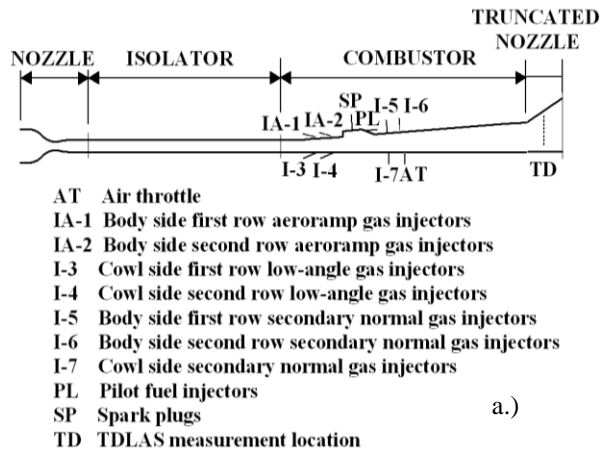


Figure 2. Schematic of the combustor flow path a.) and the aeroramp injector block with the cavity b.)

The recessed cavity flame holder is located at the divergent top wall, designated as the body side of the scramjet-powered vehicle. Figure 2b shows a schematic of the cavity flame holder and body-side injection sites. This flame holder spans the entire flow path width and has a forward-facing ramp to effectively interact with the shear layer originating from the cavity leading edge. The cavity has a length-to-depth ratio (L_{cav}/D) of 5 for the present study. Two conventional spark plugs, located at the base of the cavity, are used as the baseline ignition source.

There are eight cavity fuel injectors located at the cavity ramp to provide cavity fuel injection parallel to the cavity base. The body side injectors (I-1, I-2) are banks of aeroramp injectors from the study of Jacobsen²² and a diagram showing the array angles can be seen in Figure 3 on the following page. Three banks of injectors (I-5 – I-7) installed downstream of the cavity flame holder provided secondary fueling options. The injection angle is normal to the combustor wall for the secondary fuel injectors. Combinations of these injector banks provide the potential to develop robust fueling schemes to enhance the combustor operability. The study relied on unheated ethylene as the fuel for both main injectors and cavity fueling ports.

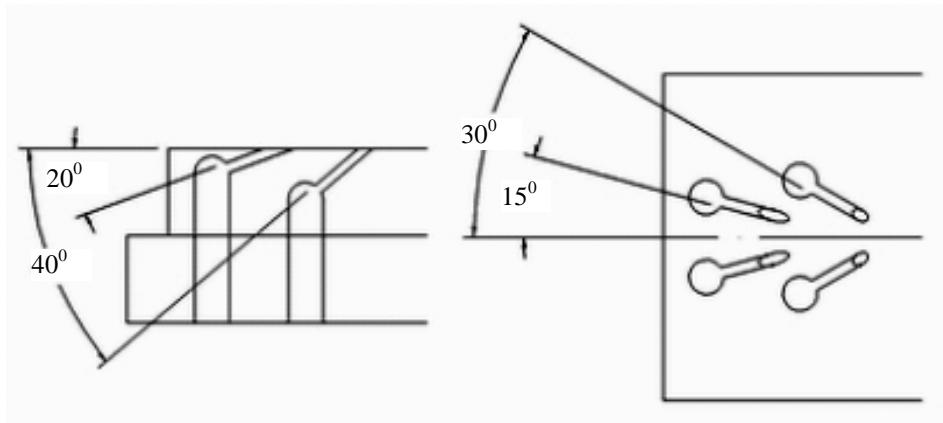


Figure 3. Aeroramp injector array Angles from the side and top ⁴

B. Data Processing

The parameters used to calculate performance and operability were: shock train position, peak pressure ratio, combustion efficiency, stream thrust, and combustor exit pressure. The shock train position was defined as where the first axial static pressure tap showed a ratio from combustor to non-combustor conditions exceeding 1.1. Peak pressure ratio is defined as the maximum static pressure, occurring at the back of the flame holder, divided by the first static pressure in the isolator. Combustor exit pressure was the average of the last two centerline taps in the combustor, one on the body (top) wall and one on the cowl (bottom) wall.

The primary performance measurement was combustion efficiency with stream thrust and exit pressure as secondary measures. Combustion efficiency was calculated using an equilibrium solver called QPERF that ran while the data was being taken. Stream thrust is defined as the thrust produced by the fluid inside the flow path.¹¹ Stream thrust and combustion efficiency with their associated uncertainty were calculated using the methods described by Smith et. al. in Ref. 10. The resulting error for the Case 1 baseline configuration, used as a representative run, can be seen in Table 2.

Table 2. Performance parameter uncertainty.¹⁰

Parameter	Bias	Precision	Total
Static Pressure	0.8%	0.5%	0.96%
Stream Thrust	1.23%	0.9%	1.52%
Comb. Efficiency	4.05%	3.0%	5.04%

III. Results and Discussion

The primary objectives were to determine the operability and performance differences between the aeroramp injector and the baseline 15 degree round injectors. Shock train position is the parameter of primary concern for operability between two runs with the ignition limits being the secondary operability criteria. Performance change is ultimately determined by a difference in the combustion efficiency of the two configurations. To support the combustion efficiency calculation, many intermediate parameters are used such as the stream thrust, the peak pressure ratio, and the combustor exit pressure.

The Mach numbers and dynamic pressures in Table 1 show the intended test conditions, but the translation of those parameters into conditions that can be tested is done before the test. The result is that the vitiator controls to a specified exit temperature and pressure. The actual conditions tested are shown in Table 3 with a brief summary of the critical data. The case numbers represent pairs of similar conditions corresponding to the intended conditions in Table 1. Run is the unique run identifier from the actual test where the three digit number represents the Julian date of the test for which all facility configurations are constant. The first one listed for each case is the baseline and the second is with the aeroramp injector installed. The pressure and temperature are the average conditions at the exit of the vitiator. Equivalence ratio (Φ) was calculated by dividing the measured combustor fuel flow rate by the calculated vitiator exit mass flow, and normalizing by the stoichiometric fuel/air ratio for ethylene fuel.

Table 3. Test conditions and result summary

Case	Run	P _{T4} (kPa)	T _{T4} (K)	I-2 Φ	I-5/6 Φ	Total Φ	Burned Φ	Stream Thrust(N)	η _c	Shock Pos(L _{isol} /H)
1	297AW	706	1078	0.52	0.00	0.52	0.31	574	0.60	19.0
1	303AH	705	1084	0.53	0.00	0.53	0.35	592	0.65	15.2
2	297AY	702	1083	0.72	0.00	0.72	0.40	783	0.55	11.9
2	303AJ	714	1084	0.70	0.00	0.70	0.38	707	0.54	10.8
3	297AX	705	1083	0.51	0.28	0.79	0.38	703	0.48	19.0
3	303AM	705	1083	0.48	0.26	0.75	0.34	618	0.46	15.2
4	297AK	707	994	0.52	0.00	0.52	0.32	632	0.62	19.0
4	303AP	710	995	0.60	0.00	0.60	0.40	712	0.66	10.8
5	297BA	701	1083	0.50	0.28	0.78	0.36	676	0.46	19.0
5	303AU	707	1083	0.52	0.26	0.78	0.38	649	0.48	14.1
6	297AL	713	997	0.51	0.28	0.79	0.36	703	0.45	15.2
6	303AV	710	996	0.53	0.27	0.80	0.35	676	0.44	10.8
7	301AL	697	772	0.32	0.29	0.60	0.23	810	0.38	9.7
7	308AH	702	772	0.29	0.27	0.56	0.21	814	0.38	7.5
8	301AN	698	772	0.30	0.28	0.58	0.23	850	0.39	9.7
8	308AK	708	773	0.27	0.27	0.55	0.22	850	0.40	6.4
9	301AO	355	697	0.31	0.29	0.60	0.24	476	0.40	9.7
9	308AP	361	697	0.30	0.30	0.61	0.26	489	0.42	4.2
10	301AP	358	696	0.30	0.51	0.81	0.25	498	0.31	8.6
10	308AS	361	697	0.30	0.50	0.80	0.26	503	0.33	3.0
11	301AC	354	694	0.32	0.30	0.62	0.23	445	0.37	10.8
11	308AX	361	697	0.30	0.29	0.59	0.22	449	0.37	7.5
12	301AD	361	697	0.29	0.50	0.79	0.23	494	0.29	9.7
12	308AY	360	696	0.29	0.57	0.86	0.24	472	0.28	5.3

A. Operability

There were two main metrics of operability used to compare the aeroramp injector to the baseline injector: the conditions where combustion was sustained and the location of the shock train for a given combustor configuration.

i. Combustion Limits

The range of operable conditions for the aeroramp injector was significantly less than for the baseline injectors. The combustor could be ignited with the baseline injectors and an aeroramp for virtually all conditions tested from Mach 3.5 to 5 and free stream equivalent dynamic pressures of 24kPa (500 psf) to 96kPa (2000 psf.) When the aeroramp was installed, it was not possible to sustain combustion at 500 psf dynamic pressure once the aeroramp was turned off. To sustain combustion at 96kPa (2000 psf) with the aeroramp it was required to light the cavity pilot first using only pilot fuel and then add the main fuel once the pilot was stabilized while the pilot was still being fueled. Once the main fuel was lit and stabilized, the pilot fuel was removed. The 96kPa (2000 psf) cases were the only cases analyzed that used any pilot fueling.

For all conditions where the aeroramp did not operate, whether at 24kPa (500 psf) or 96kPa (2000 psf) equivalent dynamic pressure, the cavity was too rich to sustain combustion. This assertion is based on the inability to achieve ignition despite the direct fueling of the cavity. Ignition with direct fueling of the cavity with no main fuel can be achieved at an equivalence ratio of about 0.01. Figure 4 shows in a Mach 2.0 flow, the aeroramp plume with its higher vorticity has a stem drawn through the cavity shear layer shown at y=0.

A similar phenomena would occur in locally subsonic flow caused by the pre-combustion shock because there is still a fuel-rich region against the cavity shear layer. The resulting high concentration of fuel in the recirculating cavity could cause a rich blowout.

A second possibility for the decreased operability range is the jet momentum of the aeroramp injector at low and high flow rates does not perform as designed. At low

flow rates jet interaction may be less than desired such that penetration is adversely affected. The resulting fuel rich boundary layer would be entrained in the cavity and cause combustion to be unsustainable. Additionally if the jet momentum is too high, it could cause the plumes from the four arrays to interact and create an aerodynamic ramp the width of the combustor rather than four independent aerodynamic ramps. This large ramp could force compression of the air above the cavity preventing any significant quantities of air from entering the cavity. This would also create a perceived fuel lean cavity scenario. The current data set that has been analyzed does not have sufficient information to conclusively determine what is happening.

ii. Isolator Margin

While the inability to maintain or initiate combustion over a broad range of fueling conditions is a significant issue, an equally important measure of operability is the ability of the combustor to not force the pre-combustion shock train out of the isolator and, in a full engine with inlet, cause an inlet unstart and likely catastrophic loss of thrust. Shock position is most commonly expressed in diameters or duct heights of isolator (L/H) remaining in front of the pre-combustion shock. When the shock position reaches 1.4 or below for this combustor, it is considered unstarted. Any unstart cases are not included in further analysis. The location of the pre-combustion shock is primarily driven by the pressure in the combustor which in turn is driven by the amount of heat being released through combustion. The comparison of shock position relative to total Φ can be seen in Figure 5.

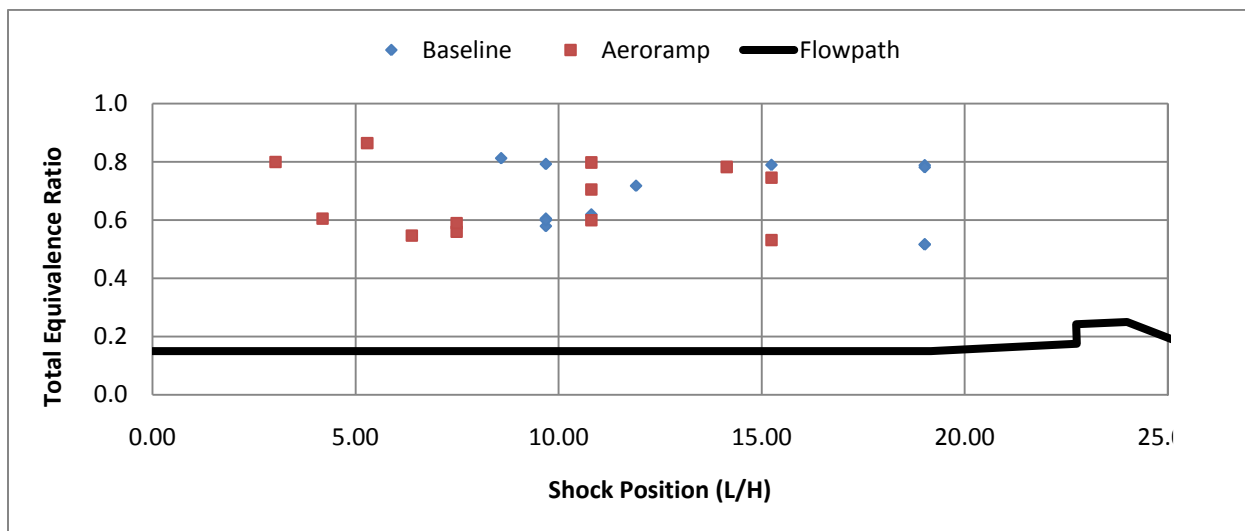


Figure 5. Shock position versus total equivalence ratio.

There is no clear correlation for the shock position versus the total equivalence ratio in either the baseline or the aeroramp. There does appear to be a trend that the aeroramp has less isolator margin than similar baseline configurations seen as a shift of the aeroramp data to the left of the baseline data in Figure 5. One reason the trend may not be strong is that some of the fuel is being injected downstream of the flame holder.

The purpose of the downstream injection is to increase the thrust at low Mach numbers while to prevent inlet unstart. Increasing the thrust is accomplished by injecting the fuel downstream of the flame holder in a section of the combustor with larger relative area. The intention is the scramjet will take over from a booster at a slower condition.¹² In order to explore this effect, the shock train position relative to only the primary fuel injection equivalence ratio was examined in Figure 6 .

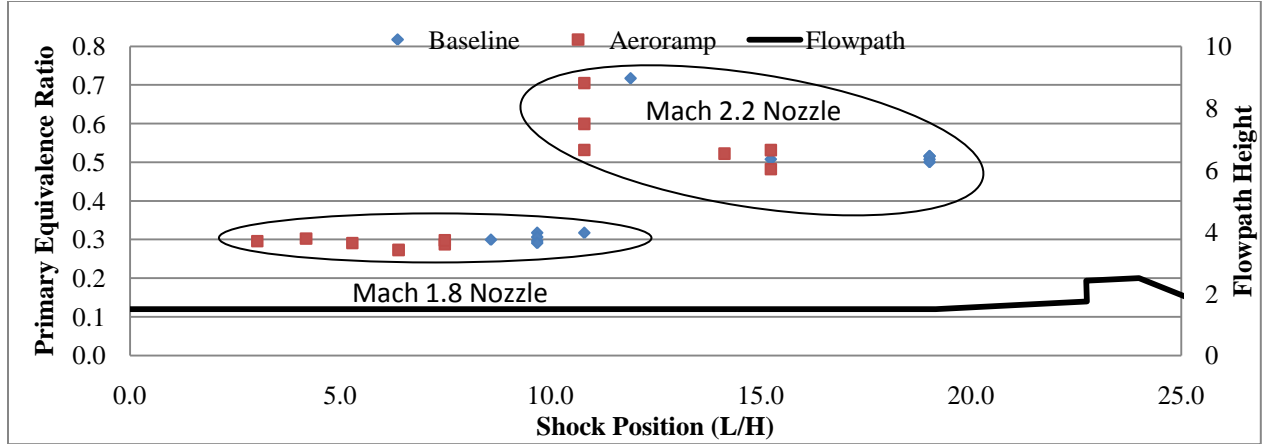


Figure 6. Shock train position versus primary (I-2) equivalence ratio.

Of note in Figure 6, the data is grouped into two sets, with the ones around a Φ of 0.3 corresponding to the Mach 1.8 facility nozzle and the higher fueling conditions correlating to the Mach 2.2 facility nozzle. For both sets, when compared to only the primary equivalence ratio, there is a very strong relationship between the baseline and the aeroramp configurations. The aeroramp has consistently less isolator margin, even to the point where the best aeroramp cases are matched with the worst baseline cases for the Mach 1.8 nozzle. The flat line of the cases with a Φ of about 0.3 show that the changes in downstream injection certainly are impacting the shock position. That is not the case of the data using the Mach 2.2 nozzle. To determine the cause of the reduced isolator margin when using the aeroramp injectors, a static pressure trace is presented in Figure 7 for Case 1. From Figure 7 the reduced isolator margin is likely caused by the higher peak pressure rise in the combustor relative to the baseline configuration.¹³

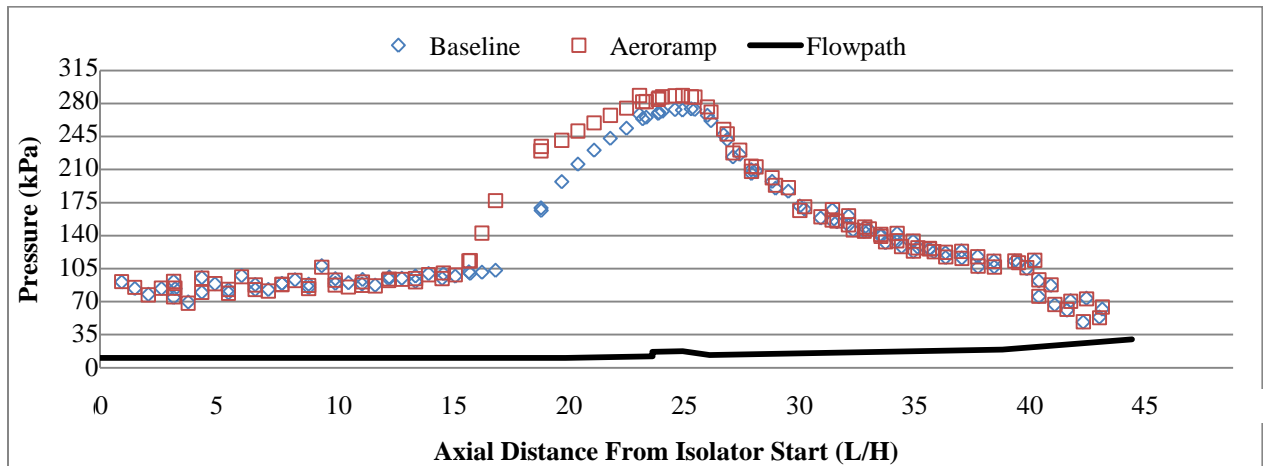


Figure 7. Axial wall static pressure (Case 1- Mach=5, Q=1000, $\Phi=0.52/0.0$).

iii. Peak Pressure Ratio

While it is likely that the reduced isolator margin in Figure 7 is due to the higher peak pressure, the difference, while outside the error, is still fairly small. The peak pressure ratios for all cases analyzed were plotted in Figure 8 to determine if Case 1 was aberration.

The peak pressure is consistently higher for the aeroramp injector. The higher peak pressure ratio is typically the result of additional combustion such as the change from Case 1 to Case 2 where the primary fuel flow is 50% greater. The absence of that variation in Cases 7-12 where the Mach 1.8 nozzle is used, indicates that the combustion process is locally very fuel rich and that as additional fuel is added, no additional enthalpy increase, and corresponding pressure rise, as result of combustion is occurring.

B. Performance

The distribution of static pressure seen in the previous section is a preliminary indicator that while the operability is different, the performance of the combustor with the two different injectors may not be significantly different. This is because in the aft portion of the combustor, where the axially oriented area is the greatest, the pressures are very similar.

iv. Combustion Efficiency (η_c)

The most obvious but complicated performance metric used to quantify engine performance is the combustion efficiency. Figure 9 shows the comparison of the combustion efficiency as a function of the total equivalence ratio for both injector configurations. Scramjet combustion efficiencies are typically in the range of 50-80% with at least 70% desired. The extremely low efficiencies seen in the higher equivalence ratios in Figure 9 make the accuracy of the inputs to the QPERF combustion efficiency calculation suspect. The online QPERF running during the test that was used to calculate the values seen in Figure 9 was compared against an offline calculation to verify the accuracy of the efficiency calculation. When the offline efficiency calculation was performed, estimates that are more accurate were made of several parameters including exit pressure and base pressure. The online efficiency uses only one of the two static pressure taps near the exit of the combust so for the offline comparison an average of the last station taps was used. Another area that the assumptions were improved is the base force calculation. The online calculation uses the true average of 12 base pressure taps, but the actual area of the base is highly weighted toward six of those taps. For the offline case, it was assumed that those six taps were representative of 70% of the force on the base. The final result was less than 2% different from the online calculation so it was concluded that the exit and base pressures were not the primary source of error. Another parameter that may be causing the differences is the heat flux. The current facility does not have a heat flux measurement so it has been assumed to be zero. The addition of that measurement will likely increase the accuracy of the 1-D calculations.

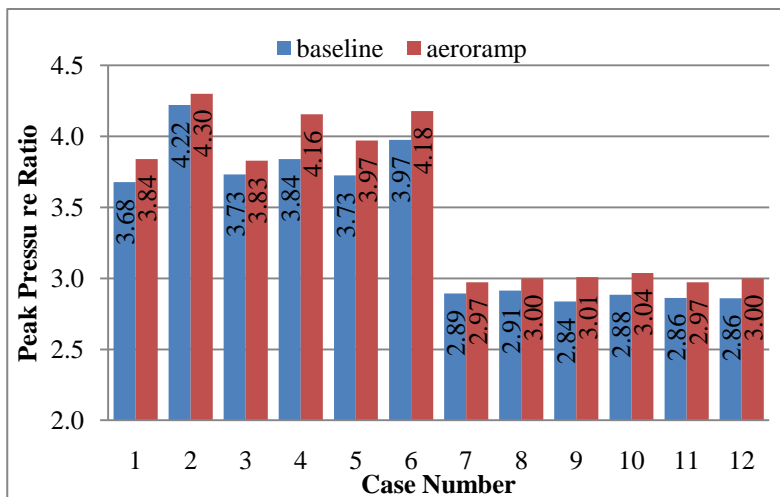


Figure 8. Peak pressure ratio comparison by case.

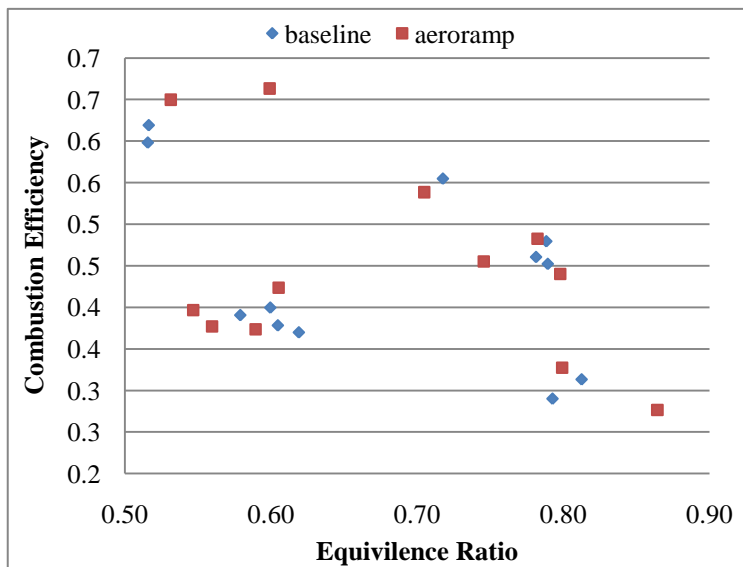


Figure 9. Combustion efficiency versus total equivalence ratio.

To determine any correlations between the data appearing in the expected 60-80% range, the same information was plotted by test case in Figure 10. The red squares are the aeroramp run for each condition. This shows that the translation from the baseline to the aeroramp configuration points is not consistent in either direction or magnitude.

The three cases with combustion efficiency above 50% are the only cases analyzed with no downstream fueling. The suggestion is the downstream fuel was not burning well, but the combustion efficiency is calculated correctly. The resulting trend (more fuel added, efficiency gets increasingly lower) also supports the hypothesis of a fuel rich downstream combustion area. The resulting low efficiencies, then, at higher equivalence ratios are reasonable. The four cases with equivalence ratios near 0.6 and efficiencies around 0.4 are the cases where the nominal equivalence ratio is 0.3/0.3 primary/secondary and the Mach 1.8 nozzle was installed. The primary equivalence ratio for these test conditions was near a possible maximum. Figure 11 shows the shock location (as identified by the rapid pressure rise) to be near the inlet. If just a small additional amount of fuel was introduced upstream of the flame holder for the aeroramp configuration, the result would have been an unstart scramjet engine because the shock train position is very near the start of the isolator ($x=0$).

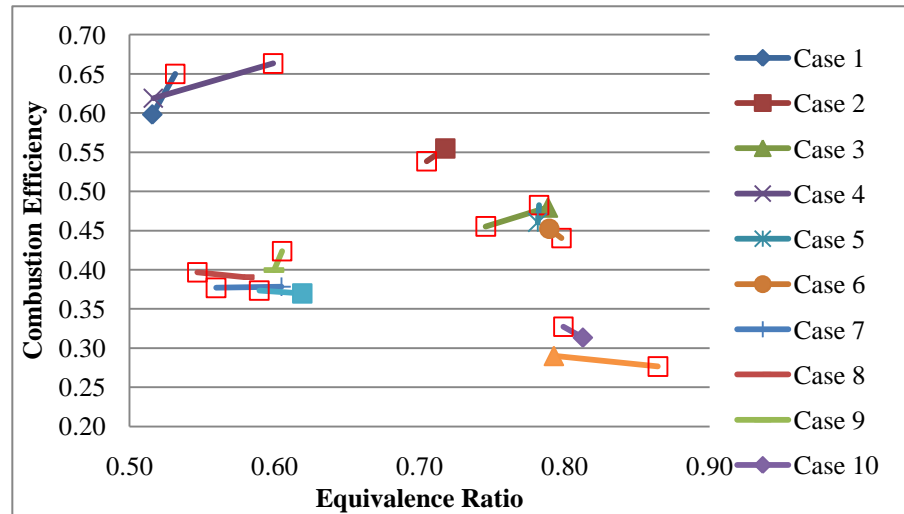


Figure 10. Combustion efficiency versus total equivalence ratio by case.

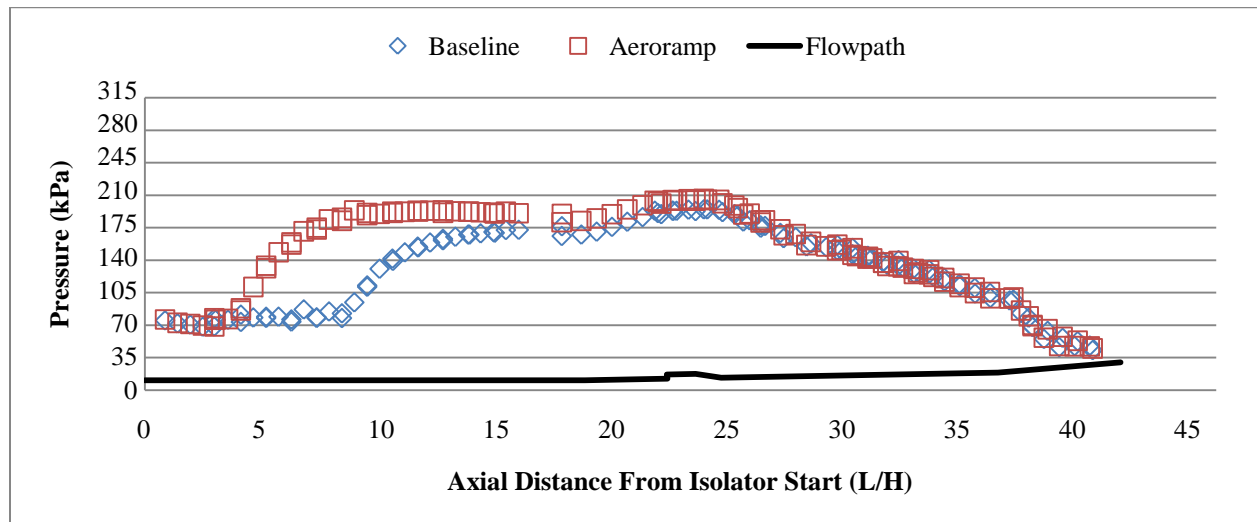


Figure 11. Wall static pressure for case 9 (Mach=3.5, $Q=1000$, $\Phi=0.3/0.3$).

The combustion efficiencies from the aeroramp and baseline configurations do not show a clear trend except for the expected decreasing combustion efficiency for increasing equivalence ratio. Figure 12 shows in some cases the aeroramp has a higher efficiency and some cases the baseline has a higher value, and all but Case 1 are easily within the ~5% error band of the analysis.¹⁰ Therefore, the combustion efficiencies are not considered statistically, significantly different between the aeroramp and the baseline.

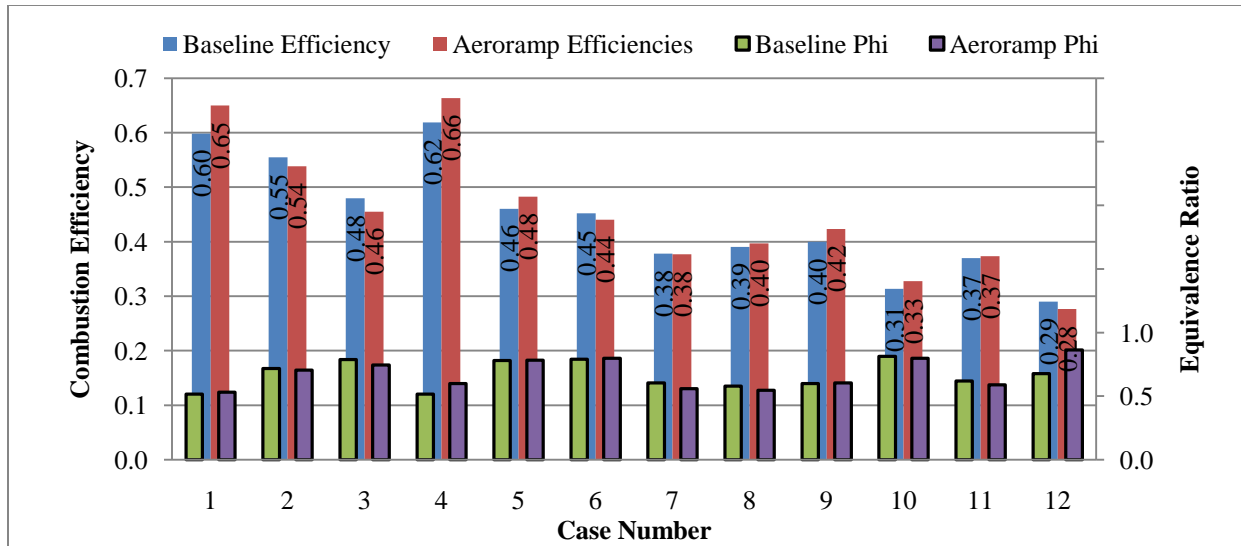


Figure 12. Combustion efficiency comparison by case.

One potential cause for the similar combustion efficiencies is that the steady-state combustion condition results in a significant portion of the flow being subsonic at the injectors due to the pre-combustion shock train. The effect of the pre-combustion shock on the fuel plume structure of two round 15-degree angled injectors in a cavity-based flame holder can be seen in Figure 13 for a single hole round injector.

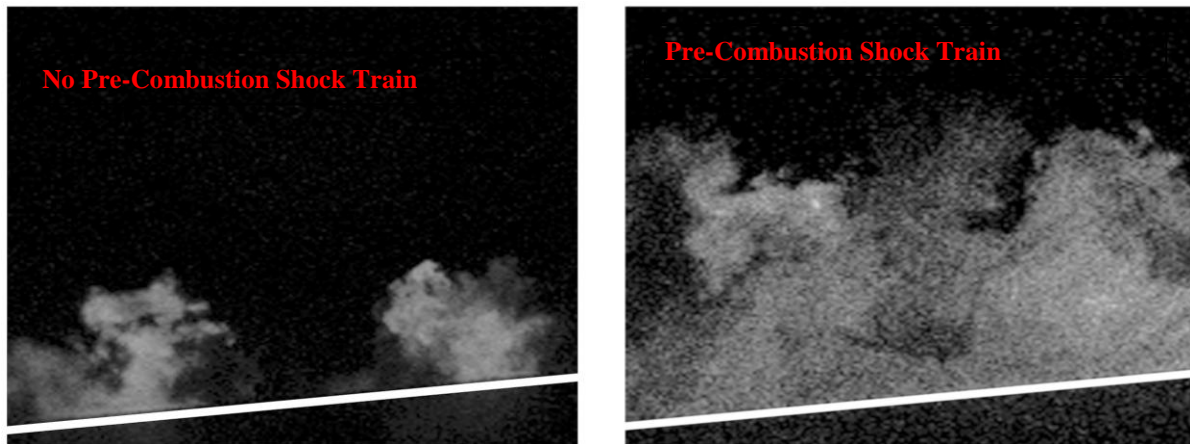


Figure 13: Instantaneous no PLIF with low/high backpressure (left/right) ¹³

The image on the left corresponds to injection into supersonic flow, the conditions that would exist before combustor ignition, the expected shape from previous work⁸. The image on the right corresponds to injection into the highly distorted flow downstream of a precombustion shock train which are the conditions that would exist after combustor ignition. This image shows the plume structure is significantly larger and better mixed. The significant increase in mixing once the combustor is started may make the aeroramp and round injectors both mix similarly. The primary benefit of the aeroramp injector is improved mixing in *supersonic* flow.

The subsonic flow field would also seem to explain why, at the end of the combustor, the aeroramp and baseline injectors give almost exactly the same wall pressures. If a different amount of fuel had been burned, the aft combustor pressures would have shifted as can be seen in the comparison of the static pressure profiles from the baseline injectors of Case 1 and Case 2 in Figure 14.

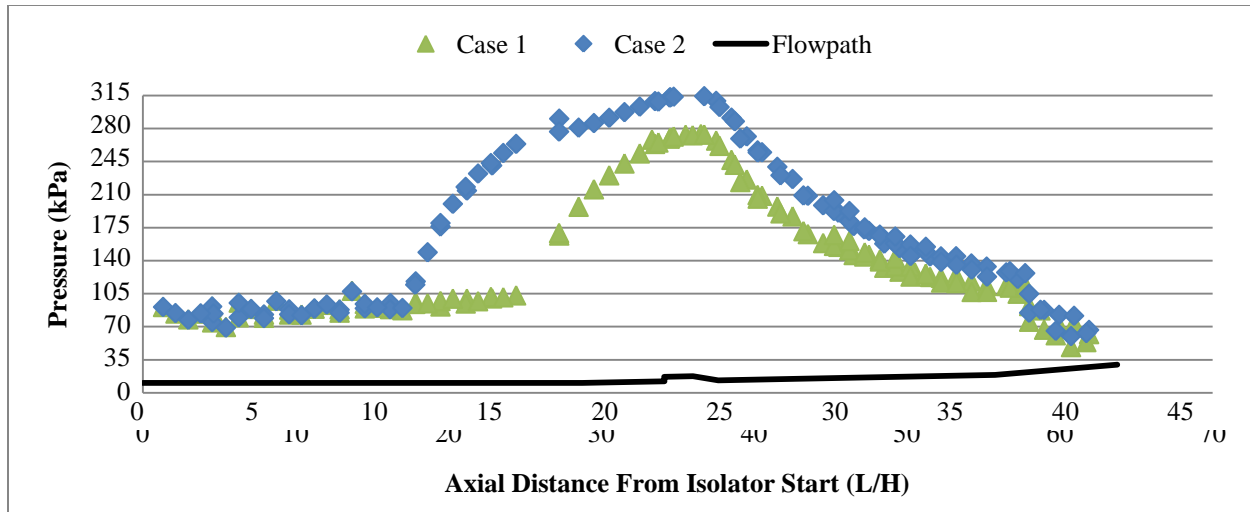


Figure 14. Axial static pressure profiles for the baseline of cases 1 and 2 (Mach=5, $Q=1000$, $\Phi=0.52$ and 0.72).

The difficulty with this hypothesis is there should not be a change in the shock position or the peak pressure rise. Therefore, the evidence supports the conclusion the aeroramp does indeed have a larger, better mixed plume. That would allow for the high pressure and temperature combustible fuel/air mixture region of the aeroramp to interact with the combustion radicals from the cavity earlier in the chamber than is the case for the round injectors. This forward movement of the flame front could cause the primary combustion region to occur in the region of the cavity rather than farther aft in the combustor where the area relief is greater. The primary combustion in the cavity region would correspond to the higher peak pressure in the cavity. Although if the same total amount of fuel was combusted, once the area was relieved, the final pressure would gradually trend to be identical. Figure 15 exhibits the pressure trend in the static pressure plot of Case 5.

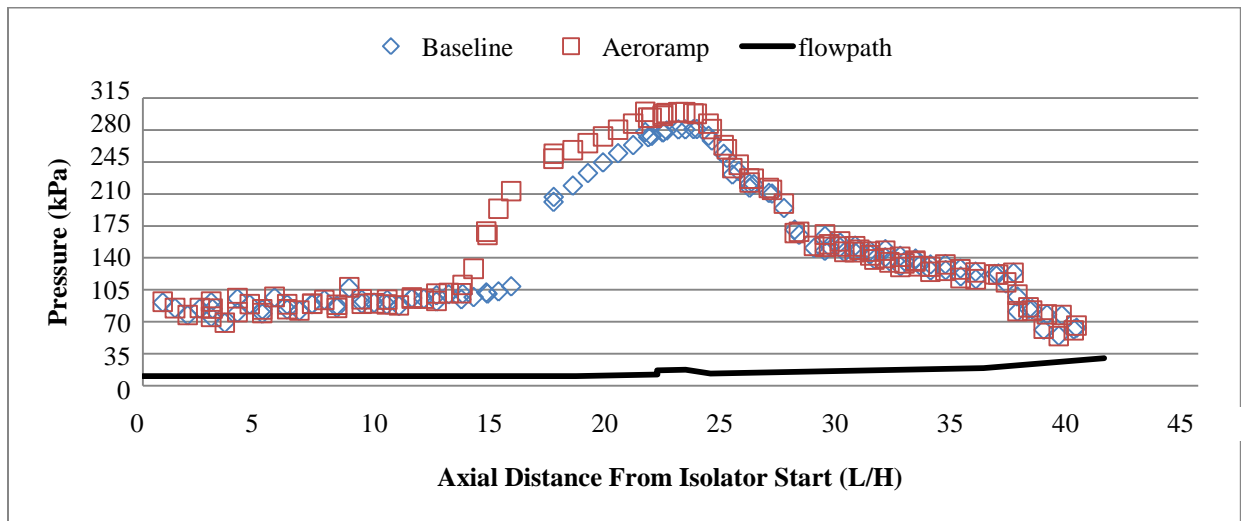


Figure 15. Axial static pressure profiles for case 5 (Mach=5, $Q=1000$, $\Phi=0.50/0.28$).

The pressures in the isolator upstream of the precombustion shock match exactly suggesting good run-to-run repeatability. The pre-combustion shock train from the aeroramp arrives earlier. The aeroramp has a higher pressure until near station 40 (downstream of the cavity flamerholder) where they again match exactly. The trend gives credence to the theory of earlier mixing and combustion, but identical total heat release. Because most of the axial differential area is in the nozzle, it is possible the thrust component of the efficiency and thus the efficiency itself is insensitive to when the combustion occurs.

Because it is suspected that the fuel injected downstream is not combusting well, the efficiency was plotted against the equivalence ratio of only the primary (I-2) fuel injector site in Figure 16.

The expected trend is that a higher efficiency will result when more of the fuel is injected upstream of the cavity. The data indicates this trend from the slight positive slope between the two sets of data in Figure 16. The lower equivalence ratio cases are for the Mach 1.8 nozzle. The steep but short trend within the Mach 1.8 nozzle grouping shows there is some effect of downstream injection. At lower Mach numbers, the low maximum equivalence ratio upstream of the flame holder, in this case about 0.30, leaves more oxygen in the flow for the downstream fuel to mix with and burn than does the higher Mach cases with twice the Φ from the primary injectors.

v. Stream Thrust

As a result of the low sensitivity to fuel injectors indicated by combustion efficiency, other parameters were used to determine where differences between the aeroramp and baseline might occur. Many of the higher sensitivity inputs to combustion efficiency are captured in the stream thrust calculation.¹⁰ Additionally, an improvement in stream thrust alone could justify tolerating a lower efficiency. The stream thrust used is the stream thrust from the combusting condition less the stream thrust at the non-combusting condition. The sensitivity of stream thrust to total equivalence ratio can be seen in Figure 17.

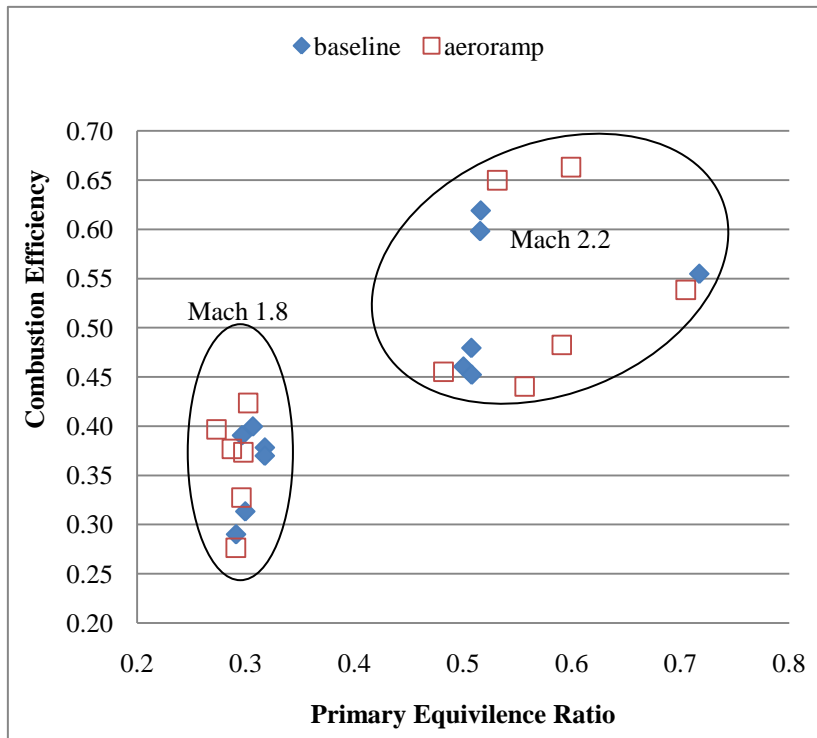


Figure 16. Combustion efficiency versus primary (I-2) fuel

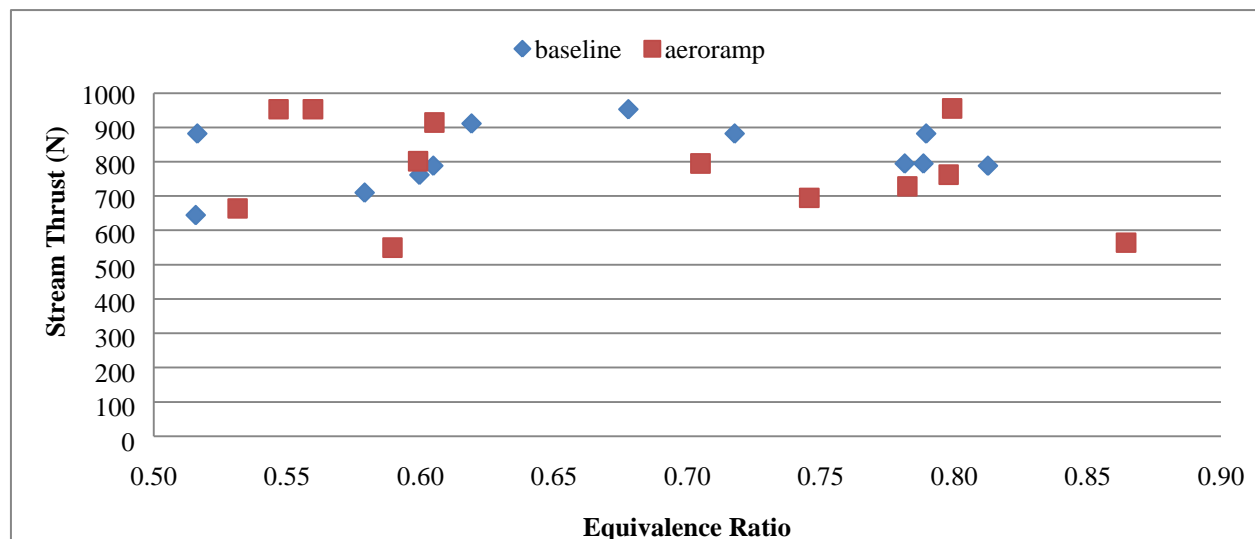


Figure 17. Stream thrust versus total equivalence ratio.

The thrust appears to be relatively constant with respect to both the type of injector and the amount of fuel. The indication is when more fuel is being added, it is not being burned, directly supporting the hypothesis that the higher

equivalence ratios are lower efficiency because the fuel is not being burned. A direct comparison of the thrust for each case can be seen in Figure 18.

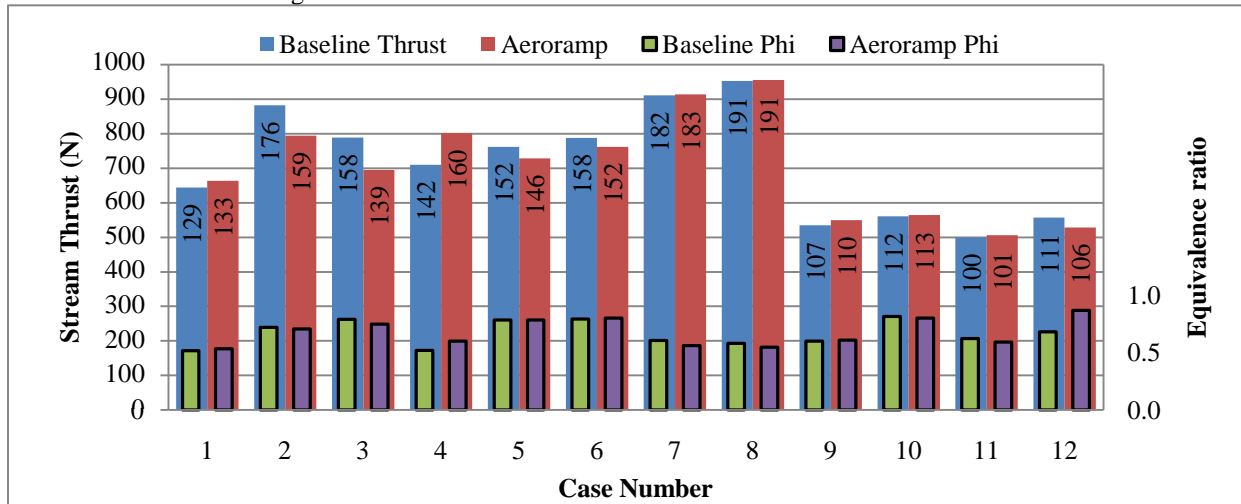


Figure 18. Combustion stream thrust comparison by case.

The direct comparison also shows there is no significant change in thrust between the aeroramp and baseline configurations. Some of the cases have a higher thrust with the aeroramp. Only some of those have a higher equivalence ratio while some actually have more thrust for less fuel. This comparison indicates the thrust is similarly inconclusive in determining any performance changes with the aeroramp injector.

The way combustion efficiency is defined in this study, it can be multiplied by the total equivalence ratio to give a parameter that is the equivalence ratio of the burned fuel. To determine if there is a similar indication of poor combustion, a comparison of the stream thrust versus Φ burned is shown in Figure 19.

There is a very strong trend showing as the amount of fuel that is being *burned* is increased, the thrust increases dramatically. This further shows that the combustion is very rich such that when the non-combusting fuel is removed from the analysis, there is a very clear trend. The aeroramp thrust appear to be slightly lower in some cases, but only slightly more than the error and not consistently.

vi. Combustor Exit Pressure

Another parameter that is directly affected by the combustion process is the combustor exit pressure. Exit pressure has a high weight in thrust because the 11-degree divergent truncated nozzle has the bulk of the axial area for the pressure force. For this paper, the combustor exit pressure is calculated as the average of the last two pressure taps in the truncated nozzle: one on the top wall and one on the bottom wall. To allow for comparisons for different inflow conditions, the exit pressure has been normalized by the first isolator pressure tap on the sidewall. A direct comparison by case is shown in Figure 20.

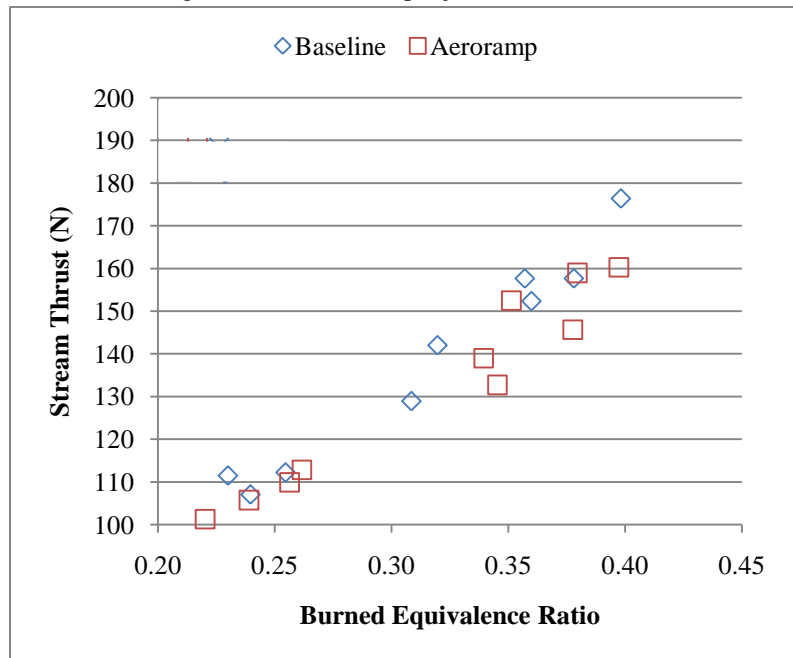


Figure 19. Stream thrust versus burned equivalence ratio.

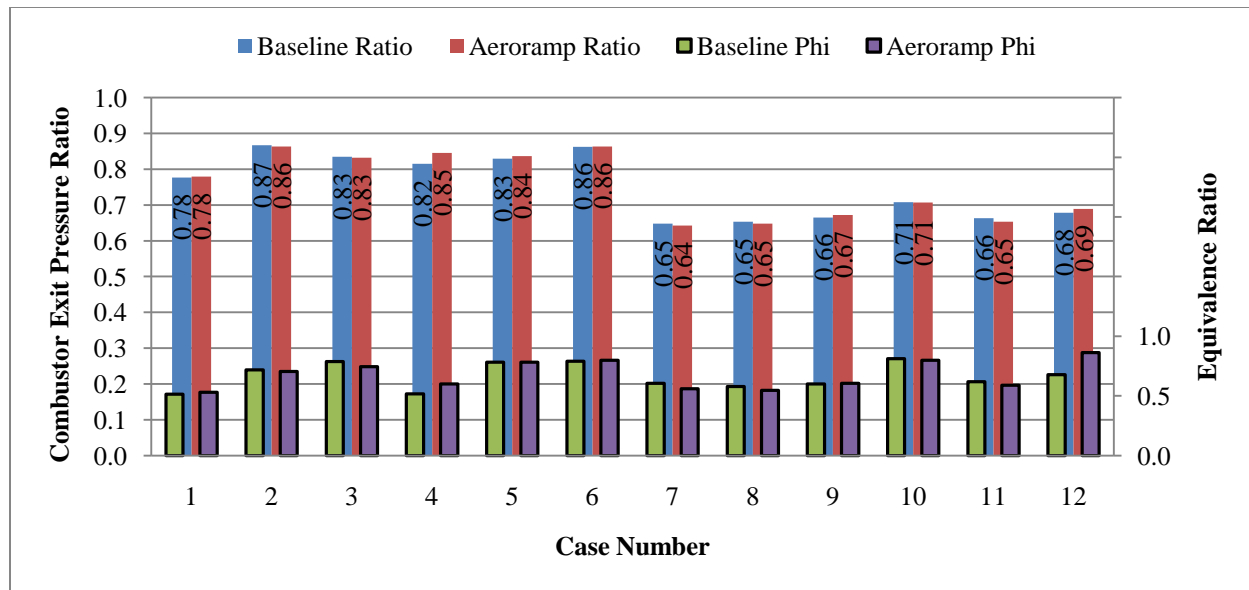


Figure 20. Combustor exit pressure ratio by case.

The data suggests two trends directly relating to the two different facility nozzles. Cases 1-6 use the Mach 2.2 nozzle and cases 7-12 use the Mach 1.8 nozzle. Within each of these groups, there is no strong sensitivity to injector type. A weak correlation to equivalence ratio is seen in the change from Case 1 to Case 2. The suggestion is increased combustion for these cases, but nothing significantly biased toward one injector over the other.

IV. Conclusions

The primary areas of interest for this study were the performance and operability implications of replacing four 15 degree round injectors with four arrays of improved aeroramp injectors. The mechanism to determine this was an experimental comparison in a dual-mode scramjet with the two different types of injectors installed at the primary injector site upstream of the flameholder. Ignition limits and pre-combustion shock position were used to define the operability differences while combustion efficiency was the primary metric used for performance comparisons.

Operability was divided into two parts: the range of conditions at which the injectors enabled sustained combustion, and the pre-combustion shock train position within the isolator for the same fuel and air conditions. The baseline fuel injector achieved sustained combustion readily at all simulated Mach numbers (3.5-5) and dynamic pressures (500-2000 psf). The aeroramp injector could not sustain combustion at any Mach number for a dynamic pressure of 500 psf. Combustion could be sustained at 2000 psf using elaborate lighting techniques, but only at a subset of the Mach range. At 1000 psf, the aeroramp could sustain combustion, but required more aerothrottle backpressure before enough combustion pressure was generated to be self sustaining. All conditions where combustion could not be sustained were due to an excessively fuel-rich cavity, even to the point of causing soot deposits on the cavity walls.

Sub-optimal operation could be characterized one of two ways. The first possible cause is the aeroramp injector arrays were not operating properly. The resulting flow field was four small jets per array unable to penetrate the boundary layer and the fuel was swept into the cavity. A second possibility is the plumes from the arrays of aeroramp injectors interacted more than the round injectors interact and prevented the incoming air from passing between the plumes. The same type of fuel rich cavity behavior would result. Finally, it is also possible the plumes left a fuel rich stem along the wall that, despite favorable mixing in the main flow, made the cavity too rich to ignite.

The ability of the isolator to contain the pressure rise from the combustor upstream of the thermal choke is critical to achieving lower Mach number operation of a dual-mode scramjet. For all fueling conditions where combustion was achieved, the aeroramp injector forced the shock train further forward than the baseline configuration at the same equivalence ratio. The most likely cause is the aeroramp injector did indeed have superior mixing causing the majority of the combustion to occur earlier in the combustor. The resulting enthalpy addition

would occur in the forward part of the combustor where the flowpath area is less, thus causing a greater pressure rise. As a result, the pre-combustion shock train moved forward reducing the operability range.

A performance criterion of scramjet combustion is the combustion efficiency. For this study, the combustion efficiency differences were generally well within the measurement uncertainty. Other performance parameters, namely the stream thrust and combustor exit pressure ratio, were analyzed more closely to shed some light on the performance differences.

All three parameters showed there was no appreciable difference in the performance of the aeroramp injector relative to the baseline injector regardless of the parameter comparison. The anticipated result is the higher pressure rise causing the reduced operability range would also cause an increase in thrust. This research indicates no additional fuel is being combusted despite the consistently higher maximum pressure ratio of the aeroramp injector. Rather, the experiments seem to merely indicate a more rapid near-field combustion process. Faster combustion is extremely desirable for scramjet mode where there is no pre-combustion shock train, but it does seem to come at a relatively steep operability penalty in dual-mode operation. This result is not entirely unexpected as the original aeroramp designs were designed and tested in a supersonic cross flow. The improved aeroramp was designed for coupling with a plasma torch igniter, which would only be used during startup, before the pre-combustion shock is formed. Further testing was in a Mach 4.0 cross flow, more indicative of the scramjet mode conditions.⁷ Operating at scramjet conditions can truly make use of the more rapid plume spreading and mixing of an aeroramp design.

The operability reduces significantly for the aeroramp injector, but the performance is virtually identical to the round injectors. Therefore, the best use of an aeroramp injector in a DMSJ configuration would likely be as an ignition aid and an upstream high Mach fuel injector. The challenge is that there will always be more complicated fabrication, and thus more risk and cost associated with an aeroramp injector, relative to a single, angled wall injector. The implication is the aeroramp should primarily be considered where the near field mixing of a round injector is insufficient to sustain combustion.

Acknowledgements

The authors acknowledge the combined energies of the AFRL/RZA management of Dr. T. Jackson, Dr. M. Lindsey Lt Col USAF, and Mr. R. Mercier for their financial and technical support of this effort. Also, the authors acknowledge the contributions of Dr. C-J. Tam, Mr. K. Jackson, Mr. P. Kennedy, Lt. J. Heaton, Mr. M. Streby, Mr. S. Enneking, and Mr. T. Bulcher for technical and operational support of the experimental research facility. Support of the AFRL/RZ Research Air Facility is also appreciated.

V. Bibliography

1. Fuller, Raymond P., Wu, Pei-Kuan, Nejad, Abdollah S and Schetz, Joseph A., "Comparison of Physical and Aerodynamic Ramps as Fuel Injectors in Supersonic Flow," *AIAA Journal of Propulsion and Power*, 1998, Vol. 14, No. 2, pp. 135-145.
2. Schetz, J. A., Thomas, R.H. and Billig, F.S., "Mixing of Transverse Jets and Wall Jets in Supersonic Flow," *Separated Flow and Jets*, 1991, pp. 807-837.
3. Lin, Kuo-Cheng, Tam, Chung-Jen, Jackson, Kevin, Kennedy, Paul and Behdadnia, Robert., "Experimental Investigations on Simple Variable Geometry for Improving Scramjet Isolator Performance," *AIAA Paper 2007-5378*, 2007.
4. Jacobsen, Lance S., Gallimore, Scott D., Schetz, Joseph A., O'Brien, Walter F. and Goss, L.P., "Improved Aerodynamic-Ramp Injector in Supersonic Flow," *AIAA Journal of Propulsion and Power*, Vol. 19, No. 4, 2003, pp. 663-673.
5. Bonanos, Aristides M., Schetz, Joseph A., O'Brien, Walter F. and Goyne, Cristopher P., "Integrated Aeroramp-Injector/Plasma-Torch Igniter for Methane and Ethylene Fueled Scramjets," *AIAA Paper 2006-813*, 2006.
6. Baurle, R. A., Fuller, R.P., White, J.A., Chen, T.H., Gruber, M. R. and Nejad, A.S., "An Investigation of Advanced Fuel Injection Schemes for Scramjet Combustion," *AIAA Paper 1998-937-939*, 1998.
7. Maddalena, Luca, Campioli, Theresa L. and Schetz, Joseph A., "Experimental and Computational Investigation of Light-Gas Injectors in Mach 4.0 Crossflow," *AIAA Journal of Propulsion and Power*, Vol. 22, No. 5, 2006, pp. 1027-1038.
8. Jacobsen, Lance S., Carter, Campbell D. and Dwenger, Andrew C., "Cavity-Based Injector Mixing Experiments for Supersonic Combustors with Implications on Igniter Placement," *AIAA 2006-5268*, 2006.

9. Bonanos, Aristides M., Schetz, Joseph A., O'Brien, Walter F. and Goyne, Cristopher P., "Scramjet Operability Range Studies of a Multifuel Integrated Aeroramp Injector/Plasma Ignitor," AIAA Paper 2005-3425, 2005.
10. Smith, S., Scheid, A., Eklund, D., Gruber, M., Wilkin, H. and Mathur, T., "Supersonic Combustion Research Laboratory Uncertainty Analysis," AIAA Paper 2008-5065, 2008.
11. Zucrow, Maurice J. and Hoffman, Joe D. *Gas Dynamics Volume I*, John Wiley & Sons, Inc, 1976, ISBN 0-471-98440-X.
12. Corbin, Christopher R., Wolff, J. Mitch and Eklund, Dean R., "Design and Analysis of a Mach 3 Dual Mode Scramjet Engine," AIAA Paper 2008-2644, 2008.
13. Gruber, Mark R., Donbar, Jeff M. and Carter, Campbell D., "Mixing and Combustion Studies Using Cavity-Based Flameholders in a Supersonic Flow," *AIAA Journal of Propulsion and Power*, Vol. 20, No. 5, 2004, pp. 769-778.